A Numerical Study of Viscous Flow Past a Thin Oblate Spheroid at Low and Intermediate Reynolds Numbers

R. L. PITTER AND H. R. PRUPPACHER

Dept. of Meteorology, University of California, Los Angeles 90024

AND A. E. HAMIELEC

Dept. of Chemical Engineering, McMaster University, Hamilton, Ontario, Canada

(Manuscript received 29 June 1972)

ABSTRACT

The flow past a thin oblate spheroid falling at terminal velocity in an infinite, viscous fluid was investigated using a numerical solution of the steady-state Navier-Stokes equations of motion. The detailed streamfunction and vorticity yielded the drag, pressure distribution, and the extent of the spheroid's downstream wake. Calculations were performed for spheroids of axis ratios 0.05 and 0.2 and Reynolds numbers between 0.1 and 100. The results were compared with other numerical and analytical solutions to the Navier-Stokes equations of motion for viscous flow past oblate spheroids and disks and with experimental results in the literature. Our numerical results for oblate spheroids of axis ratio 0.2 agree well with the numerical results of Masliyah and Epstein and with our own experimental results. Our results for oblate spheroids of axis ratio 0.05 agree well with the numerical computations of Michael and available experimental results on disks, but depart significantly from the numerical results of Rimon. In agreement with our earlier studies on spheres, we find that, as the Reynolds number approaches zero, the drag on an oblate spheroid of any axis ratio approaches its value at zero Reynolds number via the Oseen drag rather than via the Stokes drag. The significance of the present study to cloud physics is pointed out.

1. Introduction

A large amount of experimental and theoretical work has been reported in the literature on the characteristics of flow of a viscous fluid past a single sphere and on the forces between two hydrodynamically interacting spheres. In contrast, relatively little is known on viscous flow past an oblate spheroid, although numerous experimental measurements have been reported in the literature on the drag on thin disks. Thus, it is not astonishing that much is known on the collision efficiency of hydrodynamically interacting cloud drops which, for drops smaller than about 450 μ radius ($N_{Re} \leqslant 200$), can well be approximated by rigid spheres (Pruppacher and Pitter, 1971; LeClair *et al.*, 1972), while little is known on the collision efficiency of ice crystals. Jayaweera and Cottis (1969) and List and Schemenauer (1971) have shown that simple ice plates can be idealized dynamically by a circular disk. The present paper will show that the same holds true for a very thin oblate spheroid.

Wilkins and Auer (1970) have computed the collision efficiency for circular disks colliding with small spheres on the basis of the work of Ranz and Wong (1952). However, this work uses an inviscid flow model which clearly is not applicable to atmospheric ice crystals which have Reynolds numbers typically smaller than 100. In addition, we feel that it is more useful to idealize a simple ice plate, which is growing by collision with small supercooled cloud drops, by means of a thin, oblate spheroid of increasing axis ratio (AR) rather than a disk, at least in the very early states of growth. We certainly recognize that in the later stages of growth graupel particles often assume conical shapes.

As a first step to fill the need for collision efficiencies of ice crystals, we decided to obtain accurate solutions to the full, steady-state Navier-Stokes equations of motion for flow past a thin oblate spheroid with Reynolds numbers between 0.1 and 100 and with axis ratios between 0.05 and 0.2. A knowledge of the flow field around these bodies will hopefully provide a basis for future computations of the collision efficiency of simple ice plates, unrimed as well as slightly rimed.

2. Theory

a. Analytical theories

The solution to the Navier-Stokes equations of motion for the case of Stokes flow past an oblate spheroid has been discussed by Happel and Brenner (1965) on the basis of the work of Oberbeck (1876). In this flow the drag on an oblate spheroid can be expressed by the

relation[1]

$$D_{OB}=8\pi\mu V_\infty d/[\lambda_0-(\lambda_0^2-1)\cot^{-1}\lambda_0], \quad (1)$$

where $d=(a^2-b^2)^{\frac{1}{2}}$ and $\lambda_0=b/d$. If we define the drag force coefficient by

$$c_D=D/(\tfrac{1}{2}\rho_m V_\infty^2\pi a^2), \quad (2)$$

we obtain

$$c_{D_{OB}}=K/N_{\mathrm{Re}}, \quad (3)$$

with

$$K=32d/\{a[\lambda_0-(\lambda_0^2-1)\cot^{-1}\lambda_0]\}.$$

For the case of an infinitely thin, circular disk, $b\to 0$, $\lambda_0\to 0$ and $d\to a$. Thus,

$$\lim_{b\to 0} D_{OB}=16\mu a V_\infty, \quad (4)$$

$$\lim_{b\to 0} c_{D_{OB}}=\frac{64}{\pi}\Big/N_{\mathrm{Re}}=20.372/N_{\mathrm{Re}}. \quad (5)$$

As did LeClair *et al.* (1970) we found it instructive to compare drag values which were nondimensionalized with respect to the Stokes drag. From (1), (2) and (3) it follows that

$$D/D_{OB}=c_D N_{\mathrm{Re}}/K=c_D/c_{D_{OB}}. \quad (6)$$

From Eq. (6) the quantity $(D/D_{OB})-1$ can be computed which has the useful property of being equal to zero for $D=D_{OB}$. Breach (1961) used the method of matched asymptotic expansions to solve the Navier-Stokes equations of motion and generalized the results of Proudman and Pearson (1957) to apply to ellipsoids of revolution, both prolate and oblate. Using Eq. (2) to define the drag force coefficient, Breach obtained for the drag on an oblate spheroid broadside to the flow:

$$c_D=\frac{8m}{3N_{\mathrm{Re}}}\left[1+\frac{mN_{\mathrm{Re}}}{48}+\frac{m^2}{1440}N_{\mathrm{Re}}^2\ln\left(\frac{N_{\mathrm{Re}}}{2}\right)+O(N_{\mathrm{Re}}^2)\right], \quad (7)$$

with $m=12e^3\{e(1-e^2)^{\frac{1}{2}}+(2e^2-1)\tan^{-1}[e/(1-e^2)^{\frac{1}{2}}]\}^{-1}$, and $e=[1-(b/a)^2]^{\frac{1}{2}}$, the eccentricity.

For the case of an infinitely thin disk, $e=1$, Breach found

$$c_D=\frac{64}{\pi N_{\mathrm{Re}}}\left[1+\frac{N_{\mathrm{Re}}}{2\pi}+\frac{2N_{\mathrm{Re}}^2}{5\pi^2}\ln\left(\frac{N_{\mathrm{Re}}}{2}\right)+O(N_{\mathrm{Re}}^2)\right]. \quad (8)$$

If we consider in Eq. (8) only the first two terms, the expression for the drag force coefficient on a disk reduces to that obtained by Oseen (1915) for a disk, i.e.,

$$c_{DOS}=\frac{64}{\pi N_{\mathrm{Re}}}+\frac{32}{\pi^2}=\frac{20.372}{N_{\mathrm{Re}}}+3.242, \quad (9)$$

or

$$c_{DOS}=\lim_{b\to 0} c_{D_{OB}}+3.242. \quad (10)$$

As did Goldstein (1929) for the case of a sphere, Aoi (1955) obtained an exact analytical solution to Oseen's linearized equations of motion for the case of flow past a spheroid. For an oblate spheroid Aoi obtained for the drag force coefficient

$$c_D=\frac{64}{N_{\mathrm{Re}}}\frac{1}{S}\left[1+\frac{1}{2S}N_{\mathrm{Re}}\right], \quad (11)$$

where

$$S=2(\tau_0^2+1)^{\frac{1}{2}}[(1-\tau_0^2)\cot^{-1}\tau_0+\tau_0],$$

$$\tau_0=(b/a)/[1-(b/a)^2]^{\frac{1}{2}}.$$

One easily can verify that for $b\to 0$, $\tau_0\to 0$ and $S\to\pi$. For this case Eq. (11) reduces to Oseen's drag on a disk given by Eq. (9).

We shall show in this paper that all the analytical solutions mentioned above give a good approximation to the drag only at very low Reynolds numbers. For intermediate Reynolds numbers numerical solutions to the Navier-Stokes equations of motion are necessary.

b. Numerical solutions

Numerical solutions to the Navier-Stokes equations of motion have been obtained by Michael (1966) for steady viscous flow past an infinitely thin disk with $1.5\leqslant N_{\mathrm{Re}}\leqslant 50$; by Rimon (1969) and Rimon and Lugt (1969) for time-dependent flow past an oblate spheroid of axis ratio 0.05 and 0.2 and $N_{\mathrm{Re}}=10$, 100; and by Masliyah and Epstein (1970) for steady flow past an oblate spheroid of axis ratios 0.2 and 0.5 and $N_{\mathrm{Re}}=1$, 5, 10, 20, 100. Rimon showed that the work of Michael is somewhat suspect in that it does not correctly treat the sharp edge of a disk. Furthermore, it is not useful to the purpose outlined in the first section of this paper since it only considers flow past an infinitely thin disk. On the other hand, the work of Rimon and Rimon and Lugt is suspect due to the inherent difficulties in fully reaching steady-state conditions by solving the time-dependent Navier-Stokes equations of motion, and due to some numerical problems in their method of solution which showed up in their earlier treatment of flow past a sphere as discussed by Pruppacher *et al.* (1970). The best results available are those obtained by Masliyah and Epstein. Unfortunately, their work was only carried out for oblate spheroids with relatively large axis ratios and for $N_{\mathrm{Re}}\geqslant 1.0$. These deficiencies made us decide to obtain solutions to the full, steady-state Navier-Stokes equation of motion for the case of viscous flow past oblate spheroids of axis ratios lower than 0.2 and for a wider range of Reynolds numbers. For this purpose we essentially followed the numerical method of Woo (1971), adapted to oblate spheroids. Briefly, the steady-state Navier Stokes equation of

[1] See Appendix for list of symbols.

motion can be written in oblate spheroidal coordinates and in nondimensionalized form as

$$E^2(\zeta\tilde{\omega})=\frac{N_{\mathrm{Re}}}{2}\frac{\tilde{\omega}}{\mathrm{sech}^2\xi_0(\sinh^2\xi+\cos^2\eta)}J_{\xi,\eta}\left(\psi,\frac{\zeta}{\tilde{\omega}}\right), \quad (12)$$

$$E^2\psi=\zeta\tilde{\omega}, \quad (13)$$

where $\tilde{\omega}=\mathrm{sech}\xi_0\cosh\xi\sin\eta$, and where the differential operators E^2 and $J_{\xi,\eta}$ are defined by

$$E^2=\frac{1}{\mathrm{sech}^2\xi_0(\sinh^2\xi+\cos^2\eta)}\times\left[\frac{\partial^2}{\partial\xi^2}+\frac{\partial^2}{\partial\eta^2}-\tanh\xi\frac{\partial}{\partial\xi}-\cot\eta\frac{\partial}{\partial\eta}\right],$$

$$J_{\xi,\eta}(\psi,\zeta/\tilde{\omega})=\frac{\partial\psi}{\partial\xi}\frac{\partial(\zeta/\tilde{\omega})}{\partial\eta}-\frac{\partial\psi}{\partial\eta}\frac{\partial(\zeta/\tilde{\omega})}{\partial\xi}.$$

Defining the nondimensionalized quantities $G=\tilde{\omega}\xi$ and $F=\zeta/\tilde{\omega}$, the Navier-Stokes equations of motion can be written as

$$E^2G=\frac{N_{\mathrm{Re}}}{2}\frac{\cosh\xi\sin\eta}{\mathrm{sech}\xi_0(\sinh^2\xi+\cos^2\eta)}J_{\xi,\eta}(\psi,F), \quad (14)$$

$$E^2\psi=G. \quad (15)$$

Eqs. (14) and (15) were solved simultaneously by means of an IBM 360/91 or CDC 6400 electronic digital computer for the following boundary conditions:

Along the axis of symmetry: $\eta=0,\pi:\psi=0,\zeta=0$

On the surface of the spheroid: $\xi=\xi_0:\psi=0,\zeta=G/\sin\eta$

On the boundary remote from the surface: $\xi=\xi_\infty$: $\zeta=0,\psi=\frac{1}{2}\sin^2\eta\,\mathrm{sech}^2\xi_0\cosh^2\xi_\infty$.

For solving Eqs. (14) and (15) a finite-difference technique discussed by Hamielec *et al.* (1967) and Woo (1971) was used. The solutions were considered to have converged when successive values at each grid point for both the ψ and G fields had differences of less than 0.01%. From a knowledge of ψ and ζ the pressure distribution around the oblate spheroid and the drag coefficient were computed from the relations:

$$k_0=1+\frac{8}{N_{\mathrm{Re}}}\int_{\xi_0}^{\xi_\infty}\left(\frac{\partial\zeta}{\partial\eta}\right)_{\eta=0}d\xi, \quad (16)$$

$$k(\eta)=k_0+\frac{4}{N_{\mathrm{Re}}}\int_0^\eta\left[\left(\frac{\partial\zeta}{\partial\xi}\right)_{\xi=\xi_0}+\zeta_{\xi=\xi_0}\tanh\xi_0\right]d\eta, \quad (17)$$

$$c_{DP}=\int_0^\pi k(\eta)\sin2\eta d\eta, \quad (18)$$

$$c_{DF}=\frac{8}{N_{\mathrm{Re}}}\tanh\xi_0\int_0^\pi\zeta_{\xi=\xi_0}\sin^2\eta d\eta, \quad (19)$$

$$c_D=c_{DP}+c_{DF}. \quad (20)$$

3. Experiment

Experiments to determine the drag on disks of various thicknesses have been reported by Schmiedel (1928), Willmarth *et al.* (1964), Jayaweera and Cottis (1969) Stringham *et al.* (1969), List and Schemenauer (1971), and Kajikawa (1971). Unfortunately, List and Schemenauer, and Kajikawa did not report their individual measurements so that only qualitative comparison could be made with their graphs. The results of Stringham *et al.* suffer of serious boundary effects except at high Reynolds numbers. Accurate values for the drag on oblate spheroids have not been reported in the literature. In order to have experimental values for comparison with our own theoretical results and those of others, we decided to carry out such experiments ourselves.

High-precision oblate spheroids of nylon, aluminum, brass and lead alloy were manufactured for us by Thiem Industries Inc., Torrence, Calif. All spheroids had a semi-major axis of $a=0.635$ cm and axis ratios of 0.5 or 0.3. The disks had a radius of $a=0.635$ cm and a thickness $\Delta=0.05$ cm, giving a thickness-to-diameter ratio of 0.04. The spheroids and disks were allowed to fall in a large plexiglass tank of 5 m in height and 30 cm in diameter filled with either Chevron turbine-oil No. 11 or Chevron Altavis-50 oil in order to span a wide range of Reynolds numbers for the falling objects. The terminal velocity of the disks and oblate spheroids was determined by means of the method and experimental set-up described in detail by Pruppacher and Steinberger (1968). From the terminal velocity the drag force coefficient was determined for a disk from

$$c_D=2g\Delta\left(\frac{\rho_s-\rho_m}{\rho_m}\right)\Big/V_\infty^2, \quad (21)$$

and for an oblate spheroid from

$$c_D=\frac{8}{3}ga\mathrm{AR}\left(\frac{\rho_s-\rho_m}{\rho_m}\right)\Big/V_\infty^2. \quad (22)$$

The ratio of the diameter of an oblate spheroid or disk to the diameter of the oil tank was 0.042. This necessitated a small wall-effect correction for lower Reynolds numbers (Fidleris and Whitmore, 1961; McNown and Malaika, 1950).

4. Results

a. Results from analytical theories

Numerical values for the drag force coefficient for an infinitely thin disk were found from the Oberbeck formulation according to Eq. (5) and from the Oseen formulation according to Eq. (9). The results of this evaluation are plotted as curves (1) and (2) in Fig. 1. Numerical values for the drag force coefficient for an

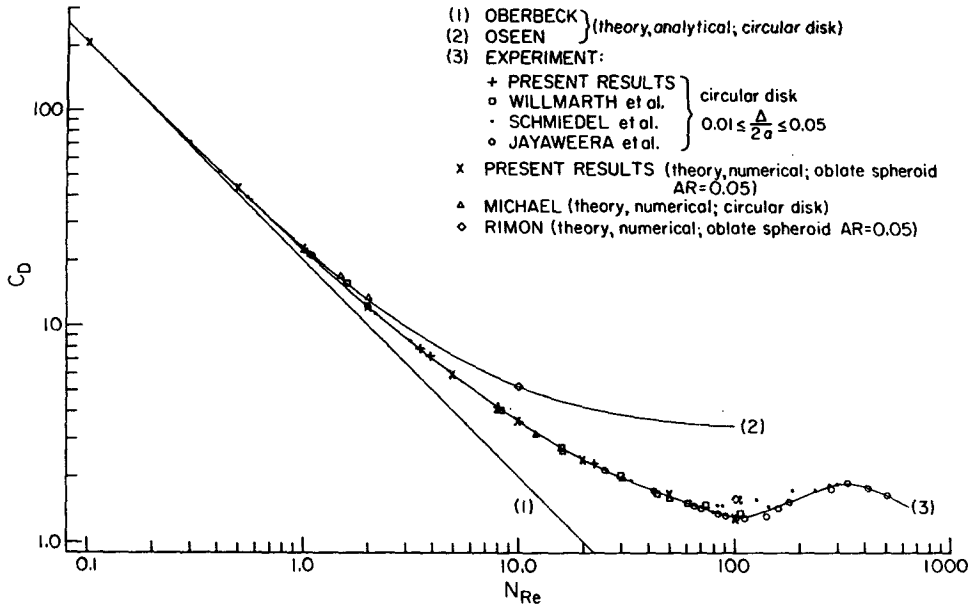

FIG. 1. Variation of the drag force coefficient with Reynolds number: comparison between various theories and experimental results for circular disks and oblate spheroids of AR=0.05.

oblate spheroid in Stokes flow were found from the Oberbeck formulation according to Eq. (3). For an oblate spheroid of axis ratio 0.05, $K=20.395$, for AR $=0.2$, $K=20.675$, for AR$=0.3$, $K=20.975$ and for AR $=0.5$, $K=21.727$. Numerical values for the drag force coefficient for an oblate spheroid of AR$=0.05$ were also found from the Aoi formulation [Eq. (11)] and the Breach formulation [Eq. (7)]. These latter results

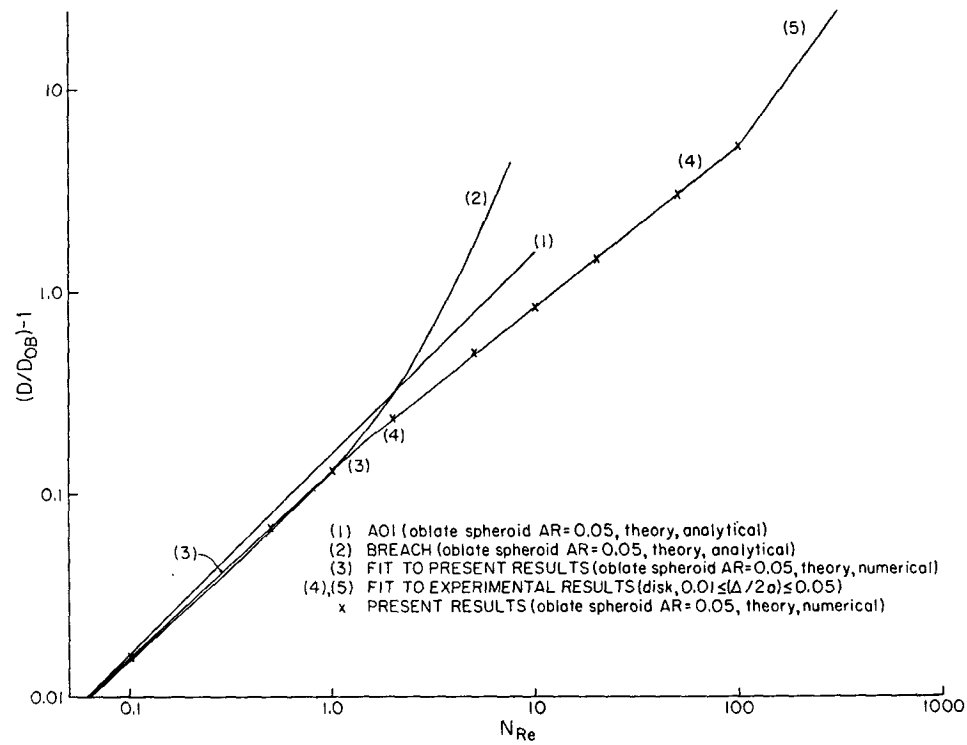

FIG. 2. Variation of $(D/D_{OB})-1$ with Reynolds number: comparison between various theories and experimental results for circular disks and oblate spheroids of AR$=0.05$.

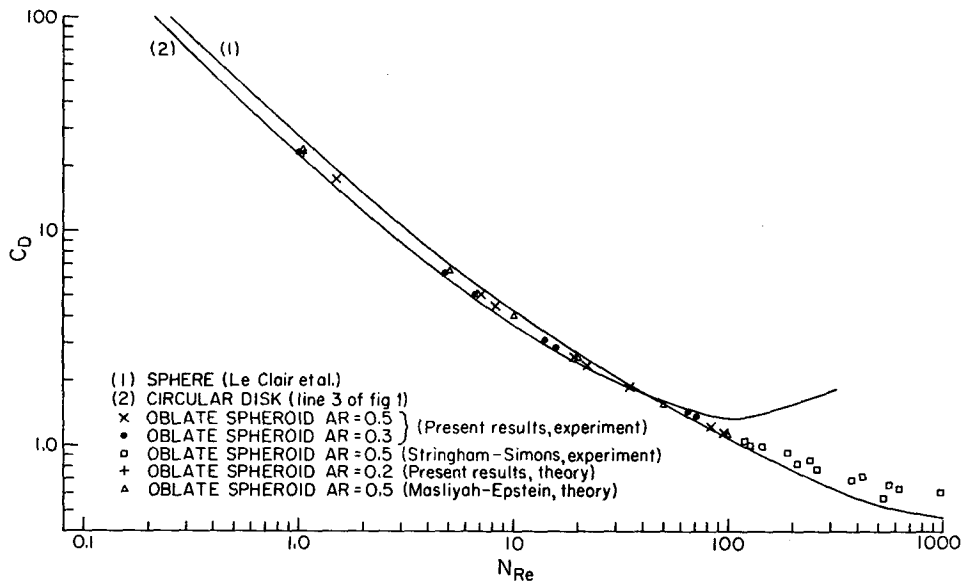

FIG. 3. Variation of the drag force coefficient with Reynolds number: comparison between theory and experimental results for oblate spheroids of AR=0.2, 0.3, 0.5.

were non-dimensionalized by the Oberbeck drag with $K=20.395$ using Eq. (6), and plotted as curves (1) and (2) in Fig. 2.

b. Results from numerical studies

The values for the drag force coefficient which we determined from our numerical analysis are listed in Table 1 as a function of step size A and B, the distance $\tilde{\omega}_\infty$ to the outer boundary, and as a function of the "mean volume" distance $\tilde{\omega}_\infty{}^*$ from the outer boundary. The quantity $\tilde{\omega}_\infty$ is found from

$$\tilde{\omega}_\infty=\cosh\xi_\infty/\cosh\xi_0,$$

where

$$\xi_0=\ln[(1+\mathrm{AR})/(1-\mathrm{AR})]^{\frac{1}{2}},\quad \xi_\infty=\xi_0+(N-1)A.$$

The quantity $\tilde{\omega}_\infty{}^*$ is defined as the ratio of the total volume of the outer envelope to the volume of the oblate spheroid all raised to the power of $\frac{1}{3}$. From the work of Masliyah and Epstein one can deduce that for thin, oblate spheroids the error in c_D due to step size is smaller than 1% if step sizes of $A=0.1$ and $B=6°$ are chosen. Two methods were used to correct for wall-effect errors. The first method was successfully used by Woo (1971) for determining the drag on a cylinder and consisted of eliminating the effects of the boundary on the flow field by extrapolating the flow field with a boundary at $\tilde{\omega}_{\infty,1}$ and the flow field with a boundary at $\tilde{\omega}_{\infty,2}$ to $\tilde{\omega}_\infty\to\infty$. This method was shown by Woo to work best at high Reynolds numbers, even with very close boundaries. At low Reynolds numbers we adopted a method which was successfully utilized by LeClair *et al.* to determine the drag on a sphere. This method involved determining c_D from a numerical solution of the complete Navier-Stokes equation of motion [Eqs. (14) and (15)] and from a numerical solution of the Stokes-flow equation

$$E^4\psi=0, \tag{23}$$

for the same two values of N, i.e., the same two values of $\tilde{\omega}_\infty$. A comparison between the drag derived numerically from the Stokes Eq. (23) for bounded flow and the drag derived analytically from the Stokes Eq. (3) for a certain N_{Re} gives an estimate for the step size and wall-effect error in c_D at that value of N_{Re}. Thus, if the subscripts indicate the equation number given in this article, the drag $c_{D_{14,15}}$ found from solving Eqs. (14) and (15) may be corrected as

$$c_{D_{\mathrm{corr}}}=c_{D_{14,15}}-(c_{D_{23}}-c_{D_3}). \tag{24}$$

Eq. (24) overcorrects c_D since the correction does not

TABLE 1. Drag force coefficient for oblate spheroids of AR=0.05 computed by present numerical method as a function of numerical parameters.

N_{Re}	A	B (deg)	N	$\tilde{\omega}$	$\tilde{\omega}_\infty{}^*$	c_D
0.1	0.1	6	49	63.8	173.2	211.1
0.1	0.1	6	61	211.8	574.9	209.8
0.1	0.1	6	49, 61	63.8, 211.8	173.2, 574.9	209.6 ($\tilde{\omega}_\infty\to\infty$)
0.5	0.1	6	49	63.8	173.2	44.1
1.0	0.1	6	61	211.8	574.9	23.21
1.0	0.1	6	49	63.8	173.2	23.23
2.0	0.1	6	49	63.8	173.2	12.67
5.0	0.1	6	49	63.8	173.2	6.17
10.0	0.1	6	15, 21	2.3, 3.9	5.9, 10.6	3.64 ($\tilde{\omega}_\infty\to\infty$)
10.0	0.1	6	49	63.8	173.2	3.87
20.0	0.1	6	15, 21	2.3, 3.9	5.9, 10.6	2.44 ($\tilde{\omega}_\infty\to\infty$)
20.0	0.1	6	49	63.8	173.2	2.63
50.0	0.1	6	21, 23	3.9, 4.8	10.6, 12.9	1.71 ($\tilde{\omega}_\infty\to\infty$)
100.0	0.1	6	21, 23	3.9, 4.8	10.6, 12.9	1.28 ($\tilde{\omega}_\infty\to\infty$)

TABLE 2. Example for the wall-effect correction method used in present numerical analysis.

N_{Re}	N	$\tilde{\omega}_\infty$	c_D [from numerical solution of Eq. (21)]	c_D [from solution of Eq. (3)]	c_D [from numerical solution of Eqs. (14),(15)]	c_D [corrected]	c_D [extrapolated]
0.1	49	63.8	210.4	203.95	211.1	204.65	
0.1	61	211.8	207.3	203.95	209.8	206.45	207.1
1.0	49	63.8	21.04	20.395	23.23	22.585	
1.0	61	211.8	20.75	20.395	23.21	22.855	23.02

TABLE 3. Corrected drag force coefficients for oblate spheroids of AR=0.05 computed by present numerical method.

N_{Re}	0.1	0.5	1.0	2	5	10	20	50	100
c_D	207.14	43.54	23.02	12.67	6.17	3.87	2.63	1.71	1.28
$(D/D_{OB})-1$	0.0156	0.0686	0.129	0.244	0.514	0.785	1.582	3.196	5.276

include inertial effects which reduce the wall effect. In order to cope with this problem we write

$$c_{D_{corr}} - c_{D_3} = (c_{D_{14,15}} - c_{D_{23}})_{\text{numerical}}. \qquad (25)$$

The right-hand side of Eq. (25) represents the inertial effect to the drag which is dependent on the proximity of the wall. From an evaluation of Eq. (25) for two values of $\tilde{\omega}_\infty$ (see Table 2), an extrapolated c_D can be derived by extrapolating the right-hand side of Eq. (25) to $1/\tilde{\omega}_\infty = 0$, as indicated in Fig. 4. The final values for c_D are listed as a function of Reynolds number in Table 3. These are plotted together with the numerical results of Michael for an infinitely thin disk and those of Rimon for an oblate spheroid of AR=0.05 in Fig. 1. In Fig. 2, our computed values for c_D are entered as $(D/D_{OB})-1$ from Eq. (6). In Figs. 5 and 6 our computed flow and vorticity fields around an oblate spheroid of AR=0.05 are displayed for $N_{Re}=1.0$ and 20. In Figs. 7 and 8 our computed values for the vorticity and pressure at the surface of an oblate spheroid of AR=0.05 are plotted for various Reynolds numbers. In Fig. 9 our computed pressure distributions around oblate spheroids of AR=0.05 and 0.2 are compared with those of Masliyah and Epstein (1970) for oblate spheroids of AR=0.2 and 0.5, and with those for a sphere given by LeClair *et al.* Our computed values for the length of the standing eddy at the downstream end of an oblate spheroid of AR=0.05 are plotted in Fig. 10 and compared with the eddy length of spheroids with axis ratios of 0.2 and 0.5 given by Masliyah and Epstein, and with the eddy length of a sphere given by Pruppacher *et al.*

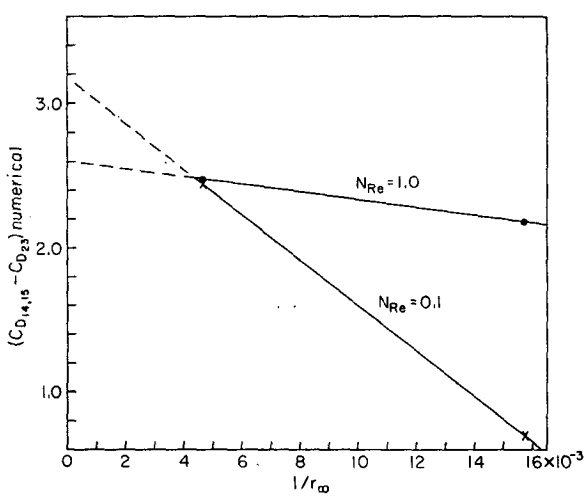

FIG. 4. Graphical determination of the boundary effect at low Reynolds numbers.

c. Results derived from experiments

From our experiments we determined c_D of a disk for five different Reynolds numbers. The values for c_D are plotted together with the experimental results of Willmarth *et al.*, Schmiedel, and Jayaweera in Fig. 1. In addition, we determined c_D of an oblate spheroid for 8 different Reynolds numbers and for AR=0.3 and 0.5. These values for c_D are plotted in Fig. 3 together with the experimental results of Stringham and Simons for oblate spheroids of AR=0.5.

5. Discussion and conclusions

1) It is seen from Fig. 1 that our computed values for the drag on an oblate spheroid of AR=0.05 agree well with the experimentally determined drag on a disk of $0.01 \leqslant (\Delta/a) \leqslant 0.05$. This agreement is even more evident from Fig. 2 which provides a sensitive test to the accuracy of the drag. From Fig. 3 we see that our computed values for the drag on an oblate spheroid of AR=0.2 agree well with those of Masliyah and Epstein for the same axis ratio. The latter, in turn, are consistent with our experimentally derived values for c_D of oblate spheroids with AR=0.3, and agree well with our experimental values for c_D of oblate spheroids with AR=0.5. The agreement between our results and those of Masliyah and Epstein (1970) is also evident

from a comparison of our computed values for the pressure at the surface of an oblate spheroid of AR=0.2

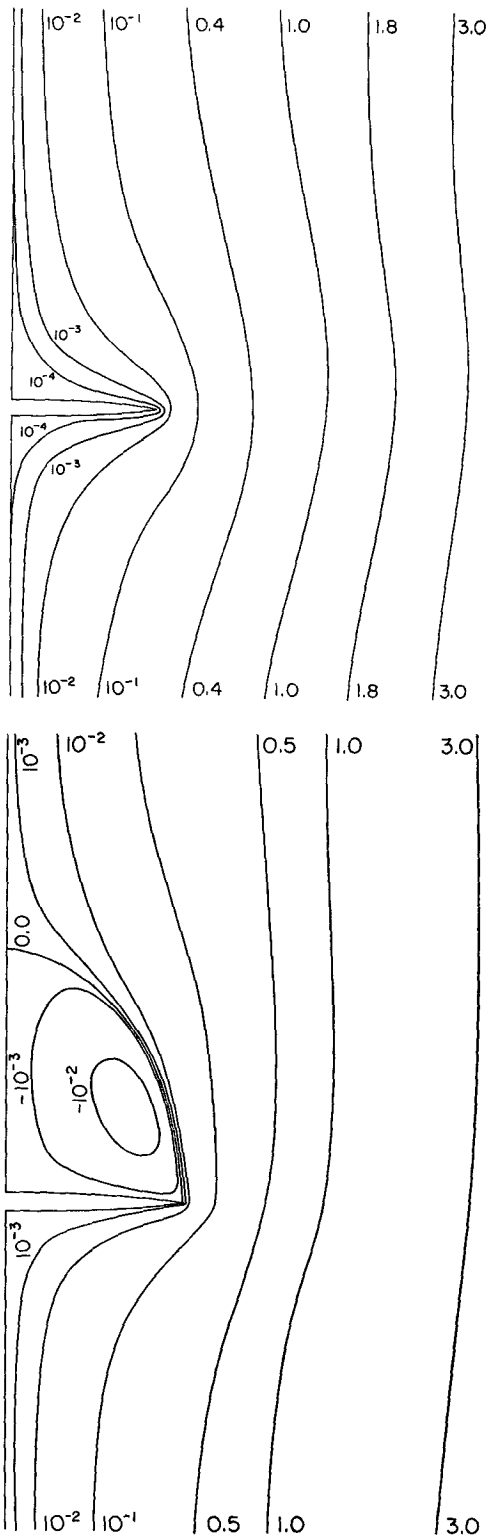

FIG. 5. Flow field around an oblate spheroid of AR=0.05, present results: upper, $N_{Re}=1$; lower, $N_{Re}=20$.

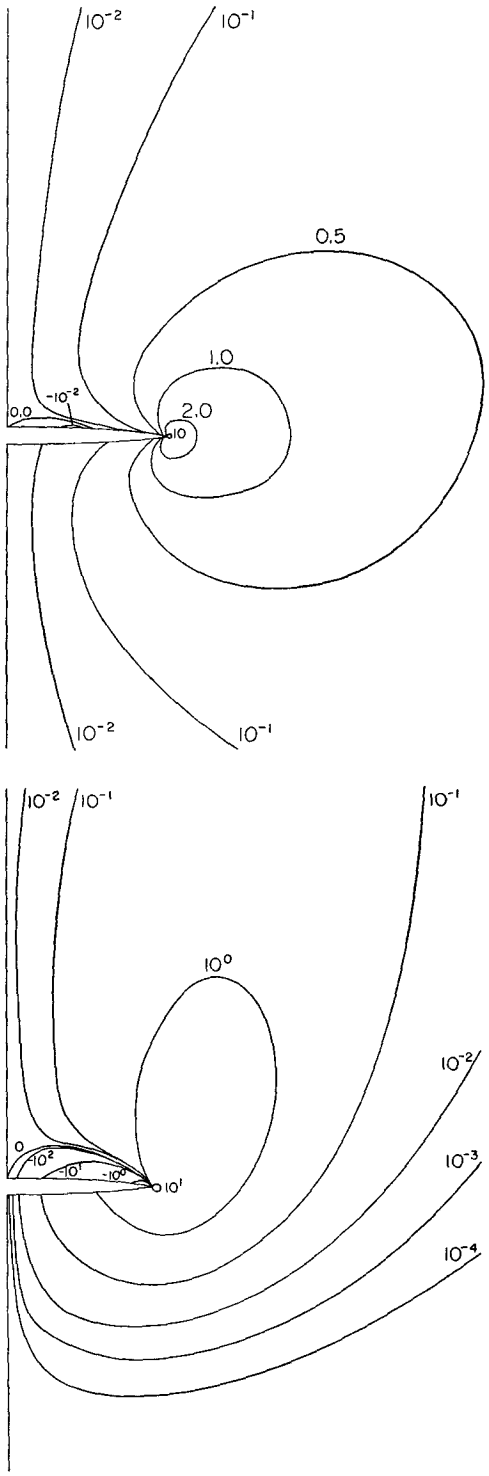

FIG. 6. Vorticity field around an oblate spheroid of AR=0.05, present results: upper, $N_{Re}=1$; lower, $N_{Re}=20$.

with the pressure distribution given by Masliyah and Epstein (Fig. 9). This evidence suggests that our method for obtaining flow fields past thin oblate spheroids is satisfactorily accurate.

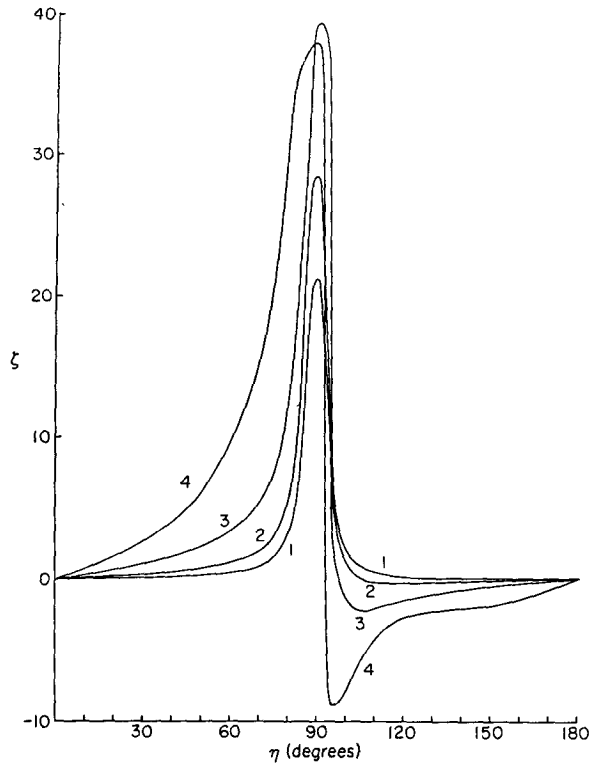

FIG. 7. Variation of the surface vorticity with polar angle and Reynolds number for an oblate spheroid of AR=0.05, present results: 1. $N_{Re}=1$; 2. $N_{Re}=5$; 3. $N_{Re}=20$; 4. $N_{Re}=100$.

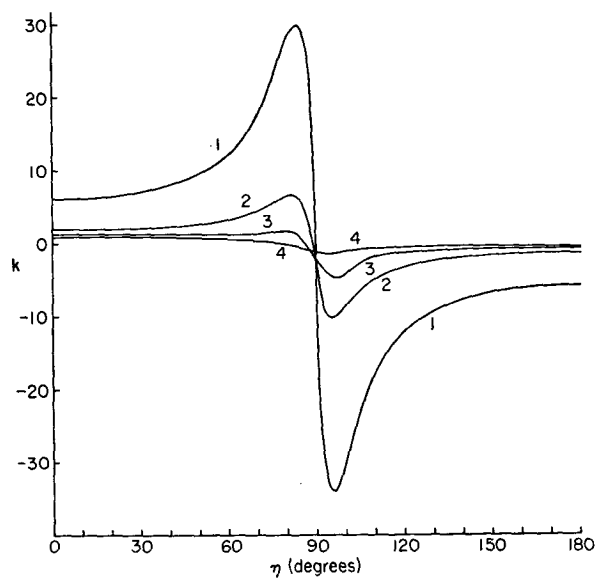

FIG. 8. Variation of the surface pressure with polar angle and Reynolds number for an oblate spheroid of AR=0.05, present results: 1. $N_{Re}=1$; 2. $N_{Re}=5$; 3. $N_{Re}=20$; 4. $N_{Re}=100$.

2) A look at Fig. 2 shows that $(D/D_{OB})-1$ on a disk or very thin oblate spheroid approaches zero via the "Oseen drag" rather than via the "Stokes' drag." This is consistent with the findings of LeClair *et al.* for spheres, and with the findings of Pruppacher *et al.* for cylinders. Thus, one might be tempted to conclude that the above statement holds for flow past objects of arbitrary shape. Furthermore, Fig. 2 shows clearly that presently available analytical solutions to the Navier-Stokes equations of motion are inadequate to describe the drag on a disk or thin oblate spheroid unless $N_{Re}<1$. The same conclusions were arrived at by LeClair *et al.* for the case of flow past spheres.

3) Fig. 2 shows further that for certain Reynolds number intervals $\log[(D/D_{OB})-1]$ of disks and thin oblate spheroids of AR$\leqslant$0.05 varies linearly with $\log N_{Re}$. It is found that for $1.5\leqslant N_{Re}\leqslant 100$

$$(D/D_{OB})-1=0.138N_{Re}^{0.792}, \tag{26}$$

and for $100\leqslant N_{Re}\leqslant 300$

$$(D/D_{OB})-1=0.00871N_{Re}^{1.393}. \tag{27}$$

Our numerical results show that at $N_{Re}=1.0$ no standing eddy has formed yet at the downstream end of an oblate spheroid of AR=0.05, while at $N_{Re}=2.0$ there is an eddy of very small extent (Fig. 10). On the other hand, it is known from experimental results (Willmarth *et al.*) that shedding of eddies from the rear of thin disks begins at $N_{Re}\approx 100$. From this result we may conclude that the "drag regimes" found are consistent with the "flow field regimes" prevalent in the flow past a disk or thin oblate spheroid, and that at the Reynolds numbers at which a flow field regime changes the drag regime also changes. The same conclusions were arrived at by Pruppacher *et al.* for the case of flow past a sphere and flow past a cylinder. Again, one

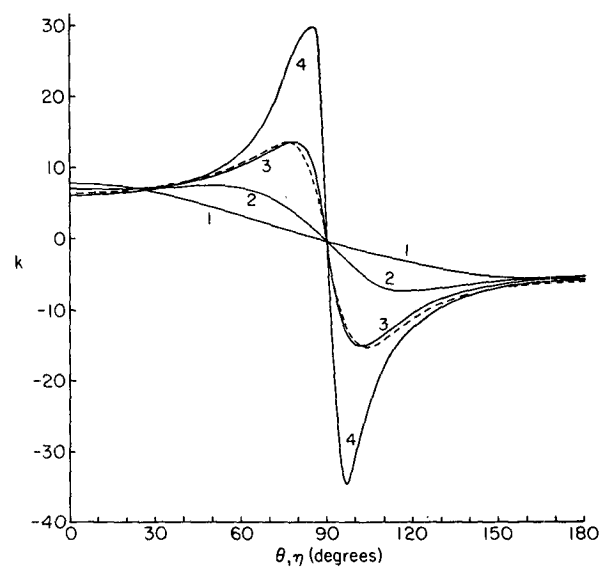

FIG. 9. Variation of the surface pressure with polar angle at $N_{Re}=1$: 1. LeClair *et al.* (sphere); 2. Masliyah-Epstein (oblate spheroid, AR=0.5); 3. Masliyah-Epstein (oblate spheroid, AR=0.2); 4. Present results (oblate spheroid (AR=0.05). Dashed line gives present results for oblate spheroid (AR=0.2).

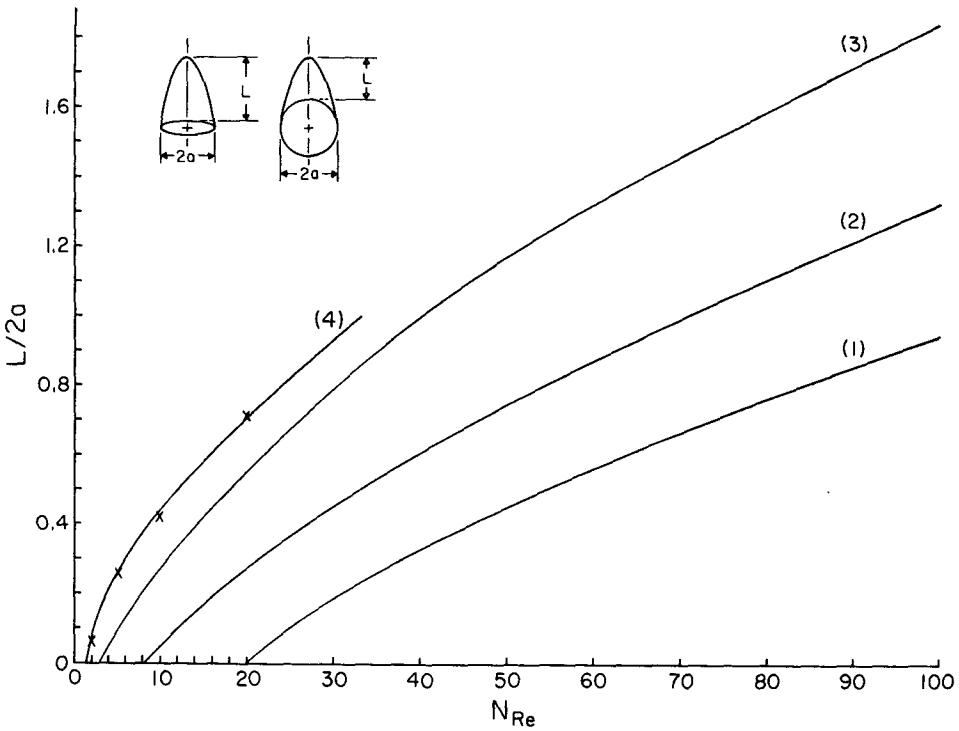

FIG. 10. Variation with Reynolds number of the length of the standing eddy at the downstream end of oblate spheroids of different axis ratio: 1. sphere; 2. Masliyah-Epstein (oblate spheroid, AR=0.5); 3. Masliyah-Epstein (oblate spheroid, AR=0.2); 4. crosses, present results (oblate spheroid, AR=0.05).

suspects that this finding is general and holds for viscous flow past a body of arbitrary shape. For $0.01 \leqslant N_{\mathrm{Re}} \leqslant 1.5$ the drag on a disk or thin oblate spheroid of AR=0.05 can be expressed by

$$(D/D_{OB})-1=10^{x}, \tag{28}$$

where

$$x=\beta_0+\beta_1 w+\beta_2 w^2, \quad w=\log N_{\mathrm{Re}},$$

with $\beta_0=-0.883$, $\beta_1=+0.906$, and $\beta_2=-0.025$. For $N_{\mathrm{Re}}<0.01$ the drag on a disk or thin oblate spheroid is given sufficiently accurate by the Oseen drag [Eqs. (7), (9) or (11)]. There are two obvious advantages in being capable of expressing the drag on a disk or thin oblate spheroid analytically as a function of the Reynolds number. First, one can easily compute the drag on such a body for any Reynolds number desired; and second, one can find the terminal velocity of such a body in a medium of any given conditions. From Eqs. (21) and (22) one finds for a disk and oblate spheroid, respectively, that

$$c_D N_{\mathrm{Re}}^2=8ga^2\Delta(\rho_s-\rho_m)/(\nu^2\rho_m), \tag{29}$$

$$c_D N_{\mathrm{Re}}^2=32ga^3(\mathrm{AR})(\rho_s-\rho_m)/(3\nu^2\rho_m). \tag{30}$$

One further finds from Eq. (6)

$$c_D N_{\mathrm{Re}}^2=KN_{\mathrm{Re}}(D/D_{OB}), \tag{31}$$

and from the definition of the Reynolds number

$$V_\infty=N_{\mathrm{Re}}\nu/2a. \tag{32}$$

Since the right-hand side of Eq. (31) is a unique function of the Reynolds number given by the analytical expressions [Eqs. (26), (27), (28), and say Eq. (9)], it is a straightforward task to derive terminal velocities for ice crystals, whose shape can be approximated by a very thin oblate spheroid or disk, for any given size a and for any given condition ν, ρ_m of the atmosphere.

Acknowledgments. Two of the authors (R. L. P. and H. R. P.) are indebted to the National Science Foundation, under Grants GA-18531 and GA-32814, and one of the authors (A. E. H.) is indebted to the Canadian Research Council, for supporting the work reported in this paper. Special thanks go to Dr. K. O. L. F. Jayaweera who graciously put at our disposal the individual values of his measurements for the drag on disks which were reported by him in literature in form of a graph as $c_D N_{\mathrm{Re}}^2$ vs N_{Re} (Jayaweera and Cottis, 1969).

APPENDIX

List of Symbols

A lattice spacing in radial direction

a radius of sphere; semi-major axis of oblate spheroid; radius of disk

AR	axis ratio of oblate spheroid, AR $= b/a$
B	lattice spacing in angular direction
b	semi-minor axis of oblate spheroid
c_D	total drag force coefficient
c_{DOS}	total drag force coefficient in Oseen-type flow
c_{DOB}	total drag force coefficient in Stokes-type flow
D	drag force of body at terminal velocity
g	acceleration of gravity
k_0	dimensionless frontal stagnation pressure $[=(p_0'-\rho_\infty')/\frac{1}{2}\rho_m V_\infty^2]$
$k(\eta)$	dimensionless stagnation pressure at angle η
L	length of standing eddy at downstream end of body
N	number of steps in radial direction
N_{Re}	Reynolds number $[=2aV_\infty/\nu]$
V_∞	terminal velocity of falling body; free stream velocity of viscous medium
Δ	thickness of disk
ψ	dimensionless stream function $[=\psi'/V_\infty a^2]$
μ, ν	dynamic and kinematic viscosity of viscous medium
ρ_m, ρ_s	density of viscous medium, density of falling body
θ	angular spherical coordinate measured from the forward stagnation point on a sphere
$\tilde{\omega}$	dimensionless radial distance from axis of symmetry $[=\tilde{\omega}'/a]$
$\tilde{\omega}_\infty$	dimensionless radial distance from axis of symmetry to outer boundary $[=\tilde{\omega}_\infty'/a]$
ξ, η	oblate spheroidal coordinates
ξ_0	value of ξ at surface of oblate spheroid
ξ_∞	value of ξ at outer boundary
ζ	dimensionless vorticity $[=\zeta' a/V_\infty]$

Primed quantities are quantities with dimensions.

REFERENCES

Aoi, T., 1955: The steady flow of viscous fluid past a fixed spheroidal obstacle at small Reynolds number. *J. Phys. Soc. Japan*, **10**, 119–141.

Breach, D. R., 1961: Slow flow past ellipsoids of revolution. *J. Fluid Mech.*, **10**, 306–314.

Fidleris, V., and R. L. Whitmore, 1961: Experimental determination of the wall effect for spheres falling axially in cylindrical vessels. *Brit. J. Appl. Phys.*, **12**, 490–494.

Goldstein, S., 1929: The forces on a solid body moving through a viscous fluid. *Proc. Roy. Soc., London*, **A123**, 216–235.

Hamielec, A. E., T. W. Hoffman and L. L. Ross, 1967: Numerical solution to the Navier-Stokes equation of motion for flow past spheres. *A. I. Ch. E. J.*, **13**, 213–219.

Happel, J., and H. Brenner, 1965: *Low Reynolds Number Hydrodynamics*. Englewood Cliffs, N. J., Prentice Hall Inc., 553 pp.

Jayaweera, K. O. L. F., and R. E. Cottis, 1969: Fall velocities of plate-like and columnar crystals. *Quart. J. Roy. Meteor. Soc.*, **95**, 703–709.

Kajikawa, M., 1971: A model study on the falling velocity of ice crystals. *J. Meteor. Soc. Japan*, **49**, 367–375.

LeClair, B. L., A. E. Hamielec and H. R. Pruppacher, 1970: A numerical study of the drag on a sphere at low and intermediate Reynolds numbers. *J. Atmos. Sci.*, **27**, 308–315.

——, ——, —— and W. Hall, 1972: A theoretical and experimental investigation of the internal circulation in water drops falling at terminal velocity in air. *J. Atmos. Sci.*, **29**, 728–740.

List, R., and R. S. Schemenauer, 1971: Free fall behavior of planar snow crystals, conical graupel and small hail. *J. Atmos. Sci.*, **28**, 110–115.

Masliyah, J. H., and N. Epstein, 1970: Numerical study of steady flow past spheroids. *J. Fluid Mech.*, **44**, 493–512.

McNown, J. S., and J. Malaika, 1950: Effects of particle shape on settling velocity at low Reynolds number. *Trans. Amer. Geophys. Union*, **31**, 74–82.

Michael, P., 1966: Steady motion of a disk in a viscous fluid. *Phys. Fluids*, **9**, 466–471.

Oberbeck, A., 1876: Über die stationäre Flüssigkeitsbewegungen mit Berücksichtigung der inneren Reibung. *J. Reine Angew. Math. (Crelle's J. Math.)*, **81**, 62–80.

Oseen, C. W., 1915: Über den Widerstand gegen die gleichmässige Translation eines Ellipsoides in einer reibenden Flüssigkeit. *Arch. Math. Phys.*, **24**, 108–114.

Proudman, I., and J. R. A. Pearson, 1957: Expansions at small Reynolds numbers for the flow past a sphere and a circular cylinder. *J. Fluid Mech.*, **2**, 237–262.

Pruppacher, H. R., and E. H. Steinberger, 1968: An experimental determination of the drag on a sphere at low Reynolds numbers. *J. Appl. Phys.*, **39**, 4129–4132.

——, B. P. LeClair and A. E. Hamielec, 1970: Some relations between drag and flow patterns of viscous flow past a sphere and a cylinder at low and intermediate Reynolds numbers. *J. Fluid. Mech.*, **44**, 781–790.

——, and R. L. Pitter, 1971: A semi-empirical determination of the shape of cloud and rain drops. *J. Atmos. Sci.*, **28**, 86–94.

Ranz, W. E., and J. B. Wong, 1952: Impaction of dust and smoke particles. *Ind. Eng. Chem.*, **44**, 1371–1380.

Rimon, Y., 1969: Numerical solution of the incompressible time dependent viscous flow past a thin oblate spheroid. Rept. No. 2955, Dept. of the Navy, Naval Ship Research and Development Center, Washington D. C., 44 pp.

——, and H. J. Lugt, 1969: Laminar flow past oblate spheroids of various thicknesses. *Phys. Fluids*, **12**, 2465–2472.

Schmiedel, J., 1928: Experimentelle Untersuchungen über die Fall Bewegung von Kugeln und Scheiben inreibenden den Flüssigkeiten. *Phys. Z.*, **29**, 593–610.

Stringham, G. E., D. B. Simons and H. P. Guy, 1969: The behavior of large particles falling in quiescent liquids. Geological Survey Prof. Paper 562-C, Gov't. Printing Office, Washington, D. C.

Wilkins, R. I., and A. H. Auer, 1970: Rimming properties of hexagonal ice crystals. *Preprints Conf. Cloud Physics*, Fort Collins, Amer. Meteor. Soc., 81–82.

Willmarth, W. W., N. E. Hawk and R. L. Harvey, 1964: Steady and unsteady motions and wakes of freely falling disks. *Phys. Fluids.*, **7**, 197–208.

Woo, S., 1971: Simultaneous free and forced convection around submerged cylinders and spheres. Ph.D. thesis, Dept. Chem. Eng., McMaster University, Hamilton, Canada.